Real-Time Analog VLSI Sensors
for 2-D Direction of Motion

Rainer A. Deutschmann[1,2], Charles M. Higgins[2] and Christof Koch[2]

[1] Technische Universität, München
[2] California Institute of Technology
Pasadena, CA 91125

Abstract. Optical flow fields are a primary source of information about the visual scene in technical and biological systems. In a step towards a system for real time scene analysis we have developed two new algorithms for the parallel computation of the direction of motion field in 2-D. We have successfully implemented these algorithms in analog VLSI hardware such that all processing is performed in the focal plane of the imager. We present data from 12×13 and 15×14 test arrays and show that the sensors are reliable for over one order of magnitude in velocity and down to 20% contrast. The algorithms allow for a very small pixel size ($110\mu m \times 110\mu m$ in a $1.2\mu m$ CMOS process) and thus high resolution arrays are feasible.

1 Introduction

Moving scenes are a rich source of information. From the optical flow important parameters such as ego-motion, time-to-contact and the focus of expansion can be inferred. Object segmentation and figure-ground segmentation based on edge detection can be improved by using discontinuities of the optical flow field.

Image motion estimation has successfully been performed in software, but high frame rates require powerful computers. More recently VLSI systems have been developed where imaging and motion computation is integrated on one single chip. In reviewing these systems, several problem areas are found. Some systems do not provide local motion information [7], some are tuned to a specific velocity [2], some systems cannot be extended to 2-D due to their algorithm [4], many sensors show poor contrast and velocity range or their output is strongly contrast dependent [7] [1]. A successful class of sensors measures time of travel of a token [6] [5] [3]. Although they show good overall performance, their extension in 2-D is difficult for algorithmical [6], wiring [5] and pixel size reasons [3]. Additionally their output either decays slowly over time [6] or is transient [5] [3].

Given that reliable 2-D velocity sensors are difficult to implement in high resolution arrays, we have developed and implemented two new algorithms for computing the local direction of motion featuring very small pixels. Our sensors are similar to biological systems in that they operate in parallel and in real time, they are power efficient, use analog as well as digital signals and are adaptive to different lighting conditions. The sensors only require nearest neighbor interaction and hold their output for a programmable time.

2 Direction of Motion Algorithms

Both sensors use the occurrence of an intensity edge at neighboring pixels as an indicator for its direction of motion. An intensity edge is detected with a temporal edge detector (TED), which we modified from [6] to respond to both dark-to-bright and bright-to-dark edges: A thresholding amplifier generates a voltage spike when a large enough temporal intensity change has occured. The voltage spike is fed into the direction of motion circuits, which we describe in sections 2.1 and 2.2 for the 1-D case. Two 1-D direction of motion units per pixel are combined for the 2-D sensor. Each pixel in the array reports the direction of motion in two tri-state currents representing the X and Y direction. A total of 9 different output combinations is therefore possible, 8 of which indicate the direction of motion in 2-D in steps of 45 degrees, the ninth indicating zero motion. The output currents persist for an adjustable time τ_{pt} after initiation before resetting themselves to zero.

2.1 Facilitate, Trigger and Compare (FTC) Algorithm

As shown in Figure 1, at the pixel position of a moving edge with the TED spike a facilitation time window is opened. Within the facilitation period τ_{fac} a TED spike from a neighboring pixel can trigger the direction of motion indicator. A comparator determines which of the directions has been triggered more recently and generates a signed constant output current accordingly, which lasts for τ_{pt}.

2.2 Inhibit-Trigger-Inhibit (ITI) Algorithm

In the ITI algorithm (see Figure 2) a TED spike triggers the output for both directions. The neighboring pixel which is next crossed by the edge then inhibits the null-direction output. The direction of motion output is computed as the difference of the two opposing directions. The ITI algorithm was inspired by [5].

3 Results

Both sensors were implemented in a standard $1.2\mu m$ analog CMOS process on 2.2×2.2mm tiny chips. We achieved pixel sizes of $128\mu m \times 119\mu m$ (FTC) and $105\mu m \times 115\mu m$ (ITI) including photoreceptor, TED and direction of motion circuitry. This allowed for a 12×13 and 15×14 pixel array, respectively. The vector field is read off the chip as two signed currents with on chip serial scanners and is displayed on a Pentium PC in video rate. The sensors themselves can operate well beyond $200\,$Hz frame rate and their real time performance will be maintained even for higher resolutions because of the parallel architecture.

In sections 3.1 and 3.2 we characterize the performance of the elementary motion detectors of the sensors. In section 3.3 we show sample snapshots of the output of the FTC sensor.

3.1 Orientation Tuning Curve

We measured the sensor response for different stimulus angles while leaving the velocity and contrast of the stimulus constant. As a stimulus we used a dark bar
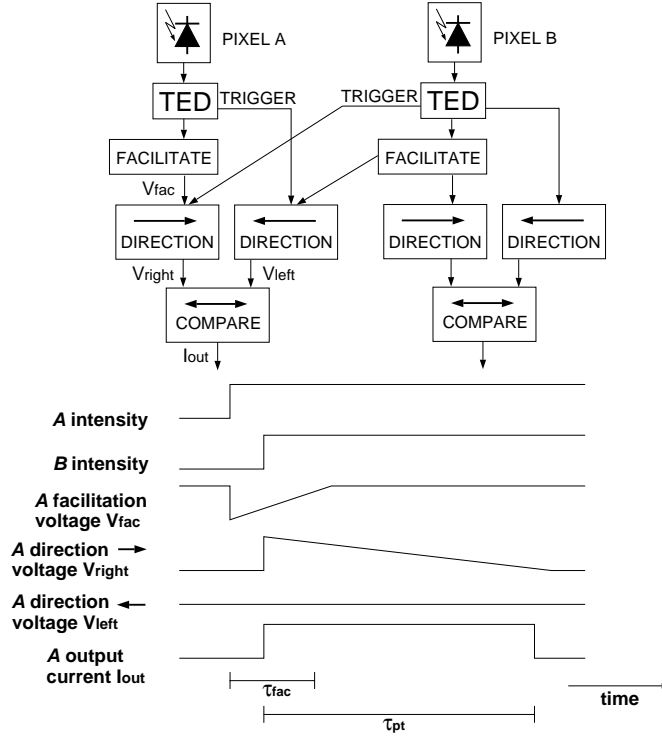
Fig. 1. FTC sensor: For an edge moving from left to right, first pixel A is facilitated and V_{fac} goes low. As the edge crosses pixel B, in pixel A the rightward motion indicator is triggered with voltage V_{right} going high. $V_{right} > 0$ and $V_{left} = 0$ in pixel A are compared and a positive output current is generated indicating that the edge moved to the right. The null-direction output is suppressed because B has not been facilitated before the leftward motion indicator in A is triggered.

on a bright background. Ideally we expect the sensor to separate the velocity space into four quadrants. For example a pixel should indicate the Y+ direction for motion in the direction anywhere from 0° to 180°, similarly the Y- direction should be indicated for stimulus motion from 180° to 360°. As can be seen in Figure 3 left, the FTC sensor performs very much like this. Because the TED misses events due to circuit noise and produces spikes of finite length, the velocity space is in fact separated into 8 directions such that for example Y+ is indicated with a probability less than one for stimulus angles close to 0° or 180°. This is most visible for the ITI sensor (see Figure 3 right).

3.2 Velocity and Contrast Range

We measured the velocity and contrast ranges over which the correct direction of motion is reported. We present data obtained for bright-to-dark edges of different contrasts and velocities (see Figure 4). The sensor output was recorded simultaneously for the whole array over multiple stimulus presentations. The output was counted as correct if the reported vector direction was within $\pm 22.5^o$
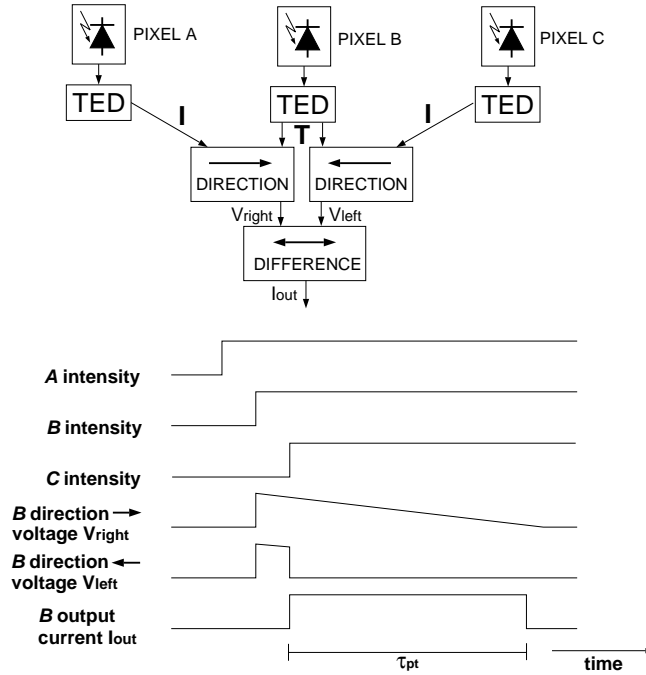
Fig. 2. ITI sensor: As pixel B is crossed by an edge moving from left to right, both V_{right} and V_{left} are triggered, but no output is reported because the difference is zero. As the edge passes pixel C, V_{left} is reset to zero and a positive current output indicating rightward motion is generated. Pixels B and A interact similarly to detect an edge moving left, producing a negative current output.

of the stimulus direction. The FTC sensor was able to report the correct direction of motion with a confidence of 90% for stimulus velocities as low as we could generate them (<25 pixels/s) and as high as 450 pixels/s for contrasts above 40%. This range spans most of the naturally relevant velocities. For high contrasts the performance is 100%. The sensor was able to respond to contrasts as low as 10%.

3.3 Flow Field Examples

In Figures 5 and 6 we present snapshots of some typical flow fields computed by the FTC sensor for natural stimuli. The data is presented as it was read off the sensor and has not been changed or thresholded in any way. The flow fields are to demonstrate the usefulness of the direction of motion sensors. For Figure 6 also the CMOS imager output is shown to clarify the underlying stimulus.
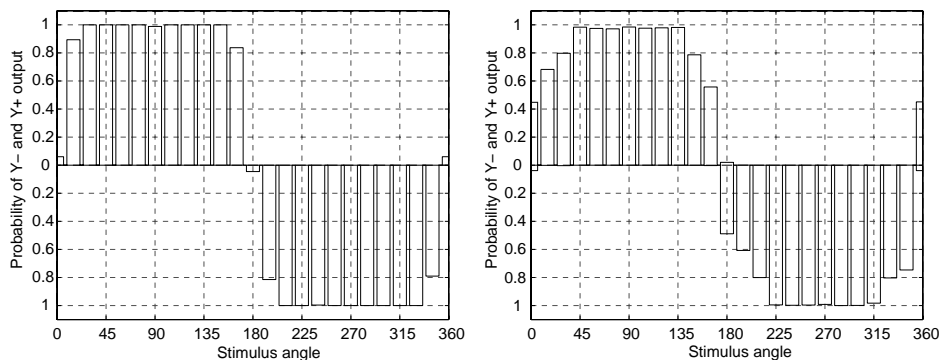
Fig. 3. Probability of Y+ output (top) and Y- output (bottom) for different stimulus angles for a high contrast stimulus shown for the FTC sensor (left) and the ITI sensor (right). Both sensors separate the velocity space reliably into four quadrants.
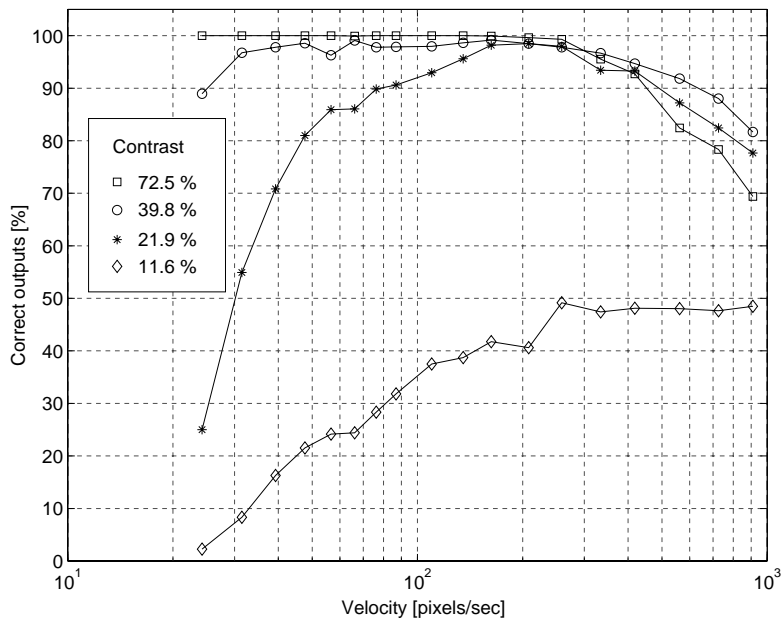

Fig. 4. Correct direction of motion output for the FTC sensor. For natural stimuli with contrasts above 40% the flow field is computed almost perfectly. For a comparable photoreceptor and TED layout the ITI sensor would yield a similar output.

References

1. A.G. Andreou, K. Strohbehn, and R.E. Jenkins. Silicon retina for motion computation. *Proc. IEEE Int. Symp. on Circuits and Systems*, 3:1373–1376, 1991.
2. T. Delbrück. Silicon retina with correlation-based, velocity-tuned pixels. *IEEE Trans. on Neural Networks*, 4:529–541, 1993.
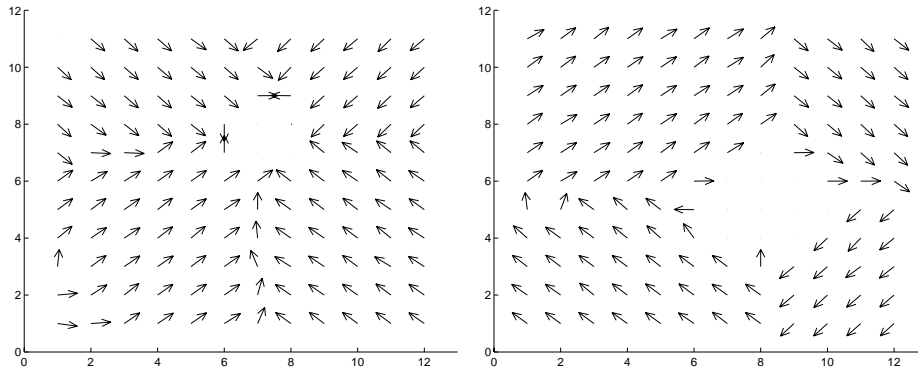
Fig. 5. FTC sensor output. The left flow field was obtained by moving a circular object away from the sensor. From the field the heading direction can be determined. The right flow field was the result for a wagon wheel pattern rotating clockwise over the sensor. Determination of the direction and axis of rotation is possible. It can be seen, as suggested by Figure 3 and expected from the algorithm, that mainly diagonal direction of motion vectors are generated.
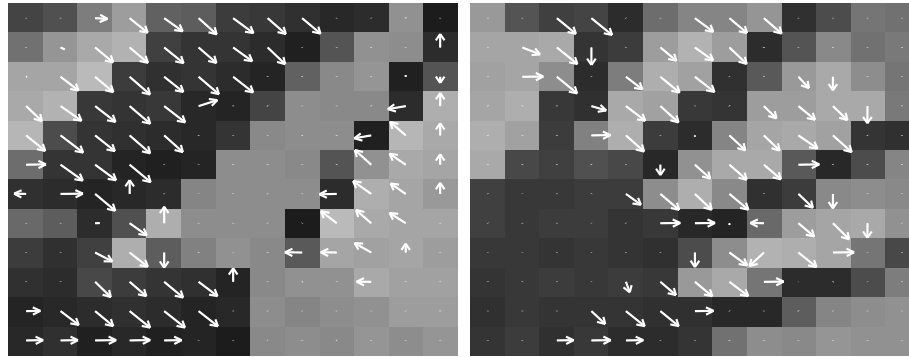

Fig. 6. FTC sensor output with underlying gray value image from the on chip CMOS imager. In the left snapshot a finger is moved right and down whereas at the same time a small pen is moved in the opposite direction. Segmentation from motion can be performed. For the right snapshot a hand was waved in front of the sensor. Even the movement of the fingers is detected.

3. R. Etienne-Cummings, J. Van der Spiegel, and P. Mueller. A focal plane visual motion measurement sensor. *IEEE Trans. Circuits and Systems 1*, 44:55–66, 1997.
4. T.K. Horiuchi, W. Bair, B. Bishofberger, A. Moore, and C. Koch. Computing motion using analog VLSI vision chips: an experimental comparison among different approaches. *Intern. Journal of Computer Vision*, 8:203–216, 1992.
5. J. Kramer. Compact integrated motion sensor with three-pixel interaction. *IEEE Trans. Pattern Anal. Machine Intell.*, 18:455–560, 1996.
6. J. Kramer, R. Sarpeshkar, and C. Koch. Pulse-based analog VLSI velocity sensors. *IEEE Trans. Circuits and Systems II*, 44:86–101, 1997.
7. J. Tanner and C. Mead. An integrated optical motion sensor. *VLSI Signal Processing II, IEEE Press*, pages 59–76, 1986.